INTEGRATION OF NEW ALIGNMENT TECHNIQUES IN THE FUTURE LHC EXPERIMENTS

J.C. Gayde & C. Lasseur
CERN, Geneva, Switzerland

The Large Hadron Collider (LHC) is CERN's new project and two proposals are reviewed for future detector systems. Detector development is mainly in two areas :

- tracking to obtain precise measurements of particle trajectories,
- muons detection in the outer layers of the detectors.

We will present a *vue d'ensemble* of some possible monitoring techniques, strongly depending on the designs, and of applied methods of determination the forms and dimensions of the future detectors.

1. ALIGNMENT PURPOSES AND FUTURE LARGE EXPERIMENTS

The aim of the alignment task is three fold :

- to ensure that the components are located properly during the construction,
- to provide geometrical information on the difference between "as built" and "the theoretical or designed " with a good accuracy,
- to monitor the detector deformations with a fine accuracy.

Two proton-proton colliding experiments are proposed namely ATLAS and CMS : the requirement of a good momentum resolution leads to the optimization of the muon alignment system which have been emphasized in both of the designs.

1.2 The ATLAS Detector (fig. 1)

It consists of an air-core magnet of 12 separate superconducting coils assembled as an axially symmetrical array around the 10 m diameter central part, each coil extending a surface area of 26 m x 5 m ; the total weight is 10500 tons. The arrangement of the muon stations follows the 12-fold symmetry of the magnet : the largest chambers are on the periphery where they span the distance of 8.5 m between two neighbouring coils ; the chambers in the middle of the field measure 5.7 m x 2 m, the inner chambers 3.2 m x 2 m. The total number is approximately 250 units in the central part [1].

1.3 The CMS Detector (fig. 2)

The overall dimensions of CMS are a length of 20 m, a diameter of 14 m and a total weight of 12000 tons. The inner part is a cylindrical volume of 7 m in length and 1.3 m in radius, the central iron part (the barrel) contains the muon chambers and is subdivided into 5 wheels (3 m in length and 14 m in diameter) of 12 regular sectors. Each sector contains four muon stations staggered to avoid pointing cracks (average : 3.5 m x 3.5 m x 0.28 m). There are 240 muon stations in the central part to be positioned and monitored [2].

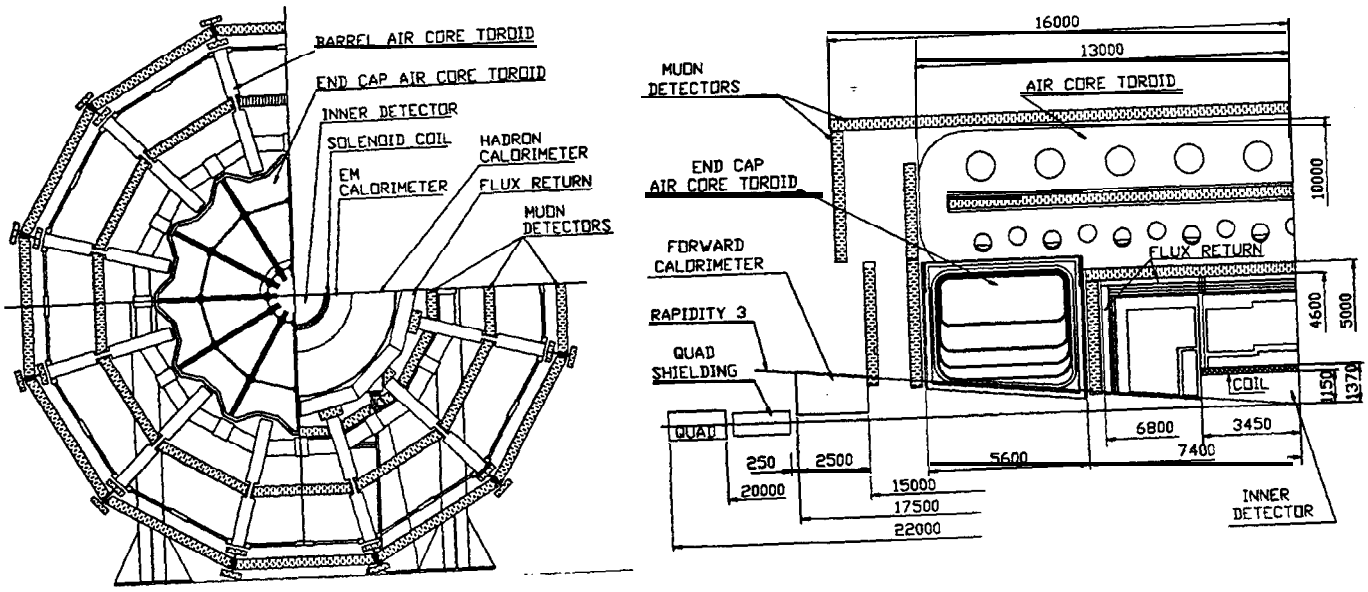

Fig 1 The Air Toroid ATLAS Detector

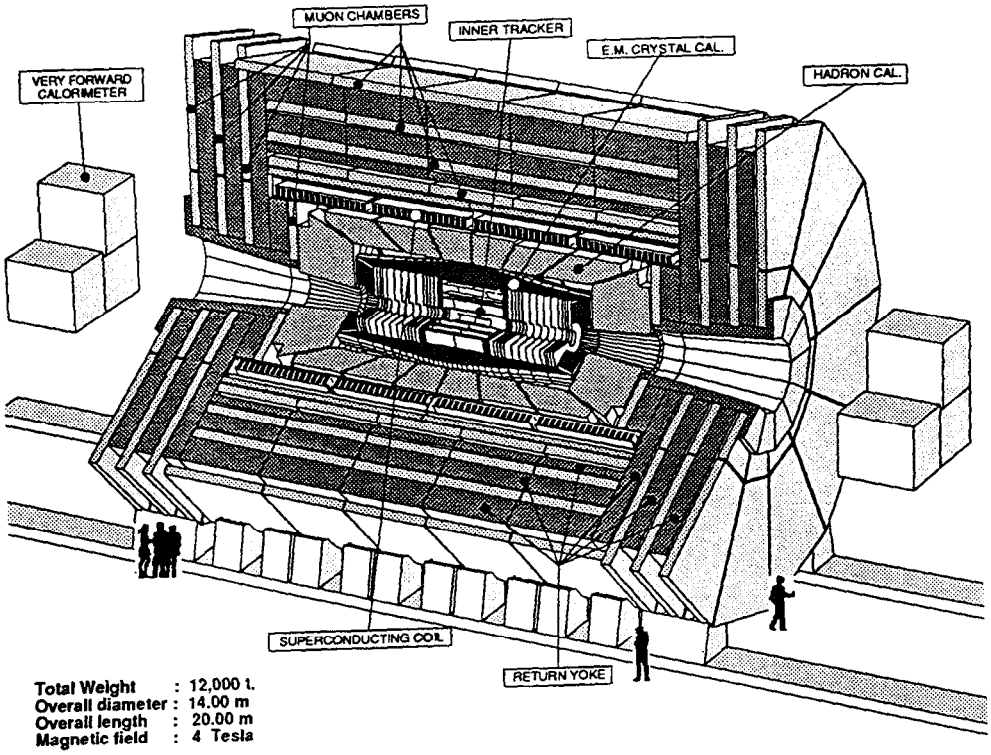

Fig. 2 The Compact CMS Detector

2. TECHNICAL CONCEPTS OF THE MUON STATIONS MONITORING

2.1 Projective Alignment System

In ATLAS, the momentum is determined by a sagitta measurement between three hits recorded in the three layers, arranged in a projective geometry, and any relative displacement of one of the three will cause a false result : the allowed misalignment must be limited to 50 μm in the bending coordinate to retain the quoted 5% momentum resolution of the muon detector.

In practice, the layers comers lie on radial lines pointing to the center of the interaction point, requiring unobstructed paths, and these lines can be materialized by light-rays simulating infinite momentum tracks : the comers carry optical elements measuring the deviation of their actual position from their nominal position on the radial lines.

2.2 "Streaming" Alignment System

The iron yoke of the CMS magnet system is part of the muon detecting system and the muon stations interleave with the iron plates. The precision for momentum measurement is considered as a 3 step operation, namely the relative position of the inner part of the experiments must be continuously monitored with a precision of 20 μm, the relative positions of the four layers of muon stations with a relative precision of 100-150 μm and the muon stations with respect to the inner part with a relative precision of 100-150 μm.

Unobstructed holes are placed in between two adjacent wheels and are occupied by the on-line alignment system which runs radially following regular lines from the inner tracking part to the outer muon layer. The system consists of optical elements which lead, control and monitor laser lights emerging from central sources up to the sensors attached to the chambers.

3. APPLIED TECHNIQUES TO THE MUON STATIONS MONITORING

3.1 Projective Alignment Techniques

They are based around optical straightness monitors which directly measure the deviation of three points from a straight line.

3.1.1 Silicon Strip Detector

Photocurrents created in 6 or 10 of photosensitive strips of 300 μm wide and 20 mm long are read out on both sides as the electronics is situated symmetrically like wings attached to the sides of a silicon crystal. The difficulties originate from any non-ideal shape of the crystal and a non uniformity of response across the strips causing a displacement of the calculated center of the beam spot. For a wave length of 1.064 μm in the Nd-YAG lasers, the absorption in silicon is 60 % for a thickness of 300 μm. The first results prove the accuracy to be 50 μm when measuring on a single strip and 10 to 20 μm can be expected with measuring on several strips **[3].**

3.1.2 Optical Straight Line Monitor

The system consists of a light emitting diode (LED) and a lens projecting a sharp image of the LED surface on a 4QD detector : tests showed that the linearity error was reduced below 5 μm over a range of ± 400 μm after calibration.

Some of the optical lengths being long (8 m) and a wider range needed to relax the static stability of the chamber structure, development using imaging technology enables to surpass the simple system : a precision coded mask (2 cm square) is illuminated and projected through the

lens onto a small CCD array (8 mm diagonal) so that any misalignment is detected after reconstructing the image and by correlating the video image to the mask template [4].

3.2 "Streaming" Alignment Techniques

By the design, the monitored lines do not follow the muon trajectories : they go through the cracks and join the tracking volume to the muon system.

The sustaining mechanical components of the alignment architecture in the central part of CMS are made of two sets free from any other detector :

- a solid structure consists of a central rigid ring placed in the middle of the detector and equipped with the laser sources plus bidirectional sensing detectors, some are fixed at systematic and accurate places in extreme planes perpendicular to the longitudinal axis, some others installed at regular positions following six axes parallel to the main longitudinal one;
- rigid tubes (3.5 m) are placed perpendicularly to the main axis and embedded in slots located in the vicinity of the muon stations comers.

From the six laser sources mounted on the central rigid ring, direct positions of the tracking volume are taken from detectors fitted at its perimeter ; its rotations are determined by six lasers installed at each extremity of the tracking volume and pointing at sensing detectors placed in the extreme perpendicular planes through six other sloped longitudinal channels.

Only one side out of the two of the stations is monitored and the external part of the corresponding tube is equipped with beam splitters transmitting light from outside monomode fibers to sensing detectors fitted on the four corners of the adjacent muon stations.

The spatial positions of the tube axes with respect to the central rigid ring are derived from data collected on the reference sensing detectors disposed on the main supports of the alignment structure and hit by the lasers emerging from the central ring [5].

A geometrical analysis package has been developed to test the abilities of the layout specially the precision of the determination of the movements of each chamber with respect to the tracking volume and accordingly to observations collected on each detector (σ 30 μm). The spatial equations of all the laser paths are established and the variations of positions on each detector versus a set of values estimated as being in the range of possible movements (a few millimeters) of the chambers are filed in an "observation chart" close to a parabolic curve.

After linearization, the value of the tangent to the curves at the origin is an expression of the effect of variations of indications given by the sensors for real variations of movements. The normalization of these variations versus the variations of the observations collected on the detectors and the covariance matrix will give the precision of determination of the movements. The results degrade from 80 μm at the bottom layer to 150 μm at the top but no physical considerations concerning the quality of the optics have been introduced yet [6].

3.3 Other and Subsidiary Alignment Techniques

Considering other alignment monitors come from the apparent need for multipoint sensing and for a redundant system as a backup for failed projective pattern and as data corroboration.

3.3.1 Nested 3-Point Optical Monitor

3-point optical monitors are "leapfrogged", such they are overlapped by half of an alignment string and the position of each component relative to the line between the initial and final monitors are derived out by a simple calculation, but the errors are propagated across the entire system and the resolution is somewhat degraded due to the mechanical errors in the

mounting of the optical elements. Investigations are performed into a precise mounting of the light source and the photosensor directly onto the lens [7].

3.3.2 Linear Capacitive Reactance Sensors

They measure the capacitive reactance of a sensor with respect to an electrically conducting object grounded with respect to the sensor.

The resolution of the stretched wire techniques surpasses 10 μm at modest cost, but the determination of wire tension and sag, the susceptibility to vibration and induced noise, the possible calibration difficulty and the mechanical fragility may entail significant risk. Nevertheless their capability of easily measuring positions and deformations plus the fact they yield redundant information make them worth to be noted [8].

The hydrostatic leveling system is designed for continuously measuring without contact vertical positions of each sensor with respect to the horizontal plane defined by the water surface : its advantages facilitate operations such as the monitoring of ground movements, displacement of heavy components, structural deformations without ground movements (thermal changes, hydraulic leaks etc.) and leveling with controlled jacks [9 & 10].

The position of a bubble gives accurate angle obtained by measuring the difference in capacitance between each sense electrode and the reference one ; the dielectric constants of the liquid and the air bubble in the vial differ by roughly 100 and this difference depends on the position of the bubble. The resolution is 1 μrad over a range of ± 0.7 mrad [11].

4. FORMS, DIMENSIONS AND DEFORMATIONS DETERMINATIONS

The stand-alone high performances of the detectors and their intricate final working positions lead the people in charge to consider further steps in the fabrication process specially regarding a more thorough knowledge of the topological structure of every module : several cubic-meters objects will be routinely and three-dimensionally measured and validated to an accuracy of a few 100 microns under simulated working conditions before they are put in their final place. To meet these needs and the inherent contingencies, new visual techniques alike the photogrammetric systems and some aspects of deformation analysis strategy are examined.

4.1 Close-Range Industrial Photogrammetry

4.1.1 State of the Art

Photogrammetry, science of image metrology, has traditionally been characterized by a rapid data acquisition phase, a lengthy film measurement and a data procession stage. Significant advances enable so-called turnkey systems employing automated film measurement through automatic monocomparators now firmly established in selected industries ; over the past few years, considerable research has been also directed towards real-time photogrammetry.

One measures not the object itself but rather photographic negatives of the object taken with one or more photogrammetic cameras from two or more locations. Since the photographed object is viewed from many different angles, the XYZ coordinates are determined from the two xy measurements on the film using the fact that the bundles of rays from each photograph intersect at the targeted object points; camera locations have not to be accurately known beforehand and the full process proves to be a very flexible technique comparing to the well-proven theodolite methods.

Photogrammetry offers quite noteworthy benefits such as accuracy, in-place measure in the desired user position, rapid data acquisition independent of targets density, reducing

downtime and minimizing effects of temperature and loading forces, permanent and irrefutable record, turnaround time for measurements as short as a few hours.

4.1.2 Accuracy Considerations

The global formula $\sigma = q\ S\ \sigma$ relates the standard errors of the XYZ coordinates σ_C to the scale of photography, 1 / S, the precision of image coordinate measurements, σ, and the factor q whose values range from an optimum of 0.4 for multi-station convergent geometries to 2.5 for weaker geometries. The form $\sigma_C = q\ d\ \sigma_a$ relates the XYZ precision directly to the standard error of angle measurement σ_a, simply determined by $\sigma_a = \sigma$ / focal length, and the average object distance, d. Both of these implicitly assume that all systematic errors (film unflatness and deformation) have been fully compensated. Another form $k = (q\ S\ \sigma / \sigma_C)^2$ gives the number of photographs per station for a desired precision [12].

Proportional accuracy in object space, estimated as σ_C / object dimension, is partly a function of both geometry and camera field of view. A standard deviation of image coordinates of 1 μm and a relative accuracy in object space of 1 / 100.000 and better is easily attainable.

Careful controls permit this high precision : large format with ultra-flat vacuum platen and back-projected reseau, 0.1 μm accuracy monocomparator with automatic video measurement of retroreflective targets, self-calibration bundle adjustment, strong networks with high convergence angles and high redundancy imaging configurations are necessary.

4.2 Approach to the Deformation Determination

4.2.1 Concept of Analysis

The determination of displacement is directly related to the choice of datum of which a change will bias the interpretation : the analysis must incorporate a scheme to determine the stable reference stations. As part of the University of New Brunswick Generalized Method, the iterative weighted S-transformation is used to alleviate the datum dependence problem ; the following procedure is adopted for two measurement epochs : determine which points form a stable reference array (the contribution of each reference station is inversely proportional to its displacement), transform the system of each of the networks into a common datum defined by the stable points, determine individual displacements within the reference system and verify that the movements constitute a statistically significant deformation [13 & 14].

4.2.2 Practical Application

As a geometrical acceptance, 180 points of a carbon fiber support (4 m x 2 m x 0.6 m) were photographed for each of the horizontal, vertical and inclined operating positions. From the results of the simulation, the camera station locations were established regarding the model and the 50 μm required 3 D accuracy : the data acquisition, using the medium format and angle (11.5 x 11.5 cm, f = 120 mm) GSI's CRC2 camera, took 30 minutes per position. The photographs were measured on the monocomparator GSI's Autoset -2 (RMS setting accuracy 0.3 μm) and the results treated with the STARS software package : for this application, the global RMS values of the XYZ coordinates were within 30 μm. The deformation analysis has been carried out by comparing the geometrical parameters of the planes and the discrete spatial reference lines measured for the diverse orientations [15].

Succeeding these tests, the model was left in an horizontal position and periodically surveyed by conventionnal triangulation : an UNB deformation analysis clearly showed the high stability of the loaded structure within 50 μm as stated to the contractor.

5. CONCLUSION

Several devices and methods are currently considered for the alignment of the muon system also for the determination of forms and real dimensions of large detection modules. Commercial products, also adapted software like PANDA, CAP, LOKAL etc., can be used whenever available and the cost trade-off is favorable.

Unfortunately, because of the stringent requirements of the operating environment, it does not appear that marketable instrumentation can be used without major modifications and adaptations; a research and development program for the alignment in the big physics detectors is being established on the basis of the output capacity from industry and the preparatory works imply close collaboration between experts of different backgrounds and the concerned firms both in the USA and in Europe.

REFERENCES

[1] Atlas Letter of Intent, CERN/LHCC 92-4 (1992).

[2] CMS Letter of Intent, CERN/LHCC 92-3 (1993).

[3] W. Blum, Muon Chamber Alignment - a Proposal, Ascot/Eagle Internal Note (1992).

[4] J. Paradiso, Analysis of an Alignment Scheme for the GEM Muon Barrel (1992).

[5] Groupe Alignement Muon CMS, Description d'un Système de Contrôle de Position des Chambres a Muons de CMS - Specifications Techniques d'un Banc Test (1993).

[6] F.Klumb, Principes de la Simulation du Dispositif d'Alignement du Projet de Détecteur CMS, AT/SU/EXP (1993).

[7] J. Govignon, Muon Detector Alignment System (1992).

[8] A. Korytov, Multi-Point Wide-Range Precision Alignment based on a Stretched Wire Technique, M.I.T (1993).

[9] D. Roux, Une Nouvelle Conception de l'Alignement - Application a l'Anneau de Stockage-de l'ESRF, Revue ESGT Mars 93 (1993).

[10] J.C. Gayde, C. Schatz, Level Tests of the Atlas Test Experiment Area in EHN2 (1993)

[11] U. Becker et al., Development of Electronic Levels (1990).

[12] C. Fraser, State of the Art in Industrial Photogrammetry, ISPRS (1988).

[13] F.J. Wilkins, Datum Definition for Deformation Analysis (1989).

[14] A. Chrzanowski et al., A General Approach to the Interpretation of Deformation Measurements, University of New Brunswick.

[15] J.C. Gayde, C. Lasseur, Dimensions et Déformations d'un Prototype Jet Cell, Atlas Internal Note (1993).